

Nonadiabatic phenomenology in small Fermi energy superconductors

L. Pietronero^{a,b}, E. Cappelluti^{a,b,*}

^a *Dipart. di Fisica, Università di Roma 'La Sapienza', P.le A. Moro, 2, 00185 Roma, Italy*

^b *Institute of Complex Systems, CNR-INFN, V. dei Taurini 19, 00185 Rome, Italy*

Abstract

High- T_c and unconventional superconductivity appears in a number of different materials with different physical properties. A common characteristics shared by almost all these compounds is that they are 'bad metal' in the sense that their effective charge carrier density is quite small, leading to a small Fermi energy E_F . In such a situation the dynamics of the electronic and lattice degrees of freedom becomes comparable ($\omega_{\text{ph}} \sim E_F$) driving these systems towards a breakdown of the Born-Oppenheimer adiabatic principle ($\omega_{\text{ph}} \ll E_F$) ruled by the comparison between the phonon frequency scale ω_{ph} and E_F . The standard concept of Fermi liquid picture applied to the electron–phonon interaction needs thus to be deeply revised. We discuss the interesting implications of the onset of nonadiabatic effects on many properties of systems with small Fermi energy.

© 2005 Elsevier Ltd. All rights reserved.

Keywords: D. Superconductivity; D. Phonons; A. Fullerenes; A. Oxides

1. Introduction

A popular concept in solid state physics is the 'quasi-particle' picture, where the highly not trivial problem of electrons interacting each other and with the lattice dynamics (phonons) is described in terms of non-interacting particles (the quasi-particles) with renormalized effective electronic parameters. This enormous simplification relies on two fundamental approximations. On one hand electron–electron interaction is usually disregarded by virtue of the Landau-Fermi liquid picture which assures the imaginary part of the electron–electron self-energy to be much smaller of the real part: $\text{Im} \sum_{\text{el}} \sim 1/\tau \ll \text{Re} \sum_{\text{el}} \sim E_F$, where τ is the electron lifetime and E_F is the characteristic electron energy scale which can be identified with the Fermi energy. On the other hand electron–ion interaction is usually treated by Born-Oppenheimer-like approximations which permit, in adiabatic regime $E_F \gg \omega_{\text{ph}}$, to separate electron and lattice degrees of freedom. Here ω_{ph} represents the characteristic energy scale of the phonon spectrum. A common feature of both of the theoretical pictures is thus the assumption of a electron energy scale much larger than any other one, $E_F \gg \omega_{\text{ph}}$, $1/\tau$, T (T being the temperature). In this situation only states close to the Fermi level ($\omega \ll E_F$) will be probed and the physical properties of

the system will not depend on the overall complex electronic structure but just on few parameters related to the Fermi level, as the electron density of states $N(0)$, the effective Fermi velocity v_F^* , the effective electronic mass m^* etc. [1].

For what concerns the electron–phonon interaction, the validity of the adiabatic hypothesis is of fundamental importance in the standard electron–phonon phenomenology, since it not only allows to describe the low energy properties of the system in terms of quasi-particles, but it defines also an exact diagrammatic theory, the Migdal–Eliashberg (ME) theory, which permits to quantify the renormalization factor for each physical properties. An interesting consequence is that almost all the relevant electron–phonon properties depend uniquely on the electron–phonon coupling constant λ , for instance [1]:

$$\frac{m^*}{m} = f_{m^*}(\lambda), \quad (1)$$

$$\frac{T_c = T_c}{\omega_{\text{ph}}} = f_{T_c}(\lambda), \quad (2)$$

$$\frac{\Omega_{\text{ph}}}{\omega_{\text{ph}}} = f_{\Omega_{\text{ph}}}(\lambda), \quad (3)$$

$$\chi = \chi_0, \text{ indep on } \lambda, \dots \quad (4)$$

where m^* is the effective electronic mass, T_c is the superconducting critical temperature, Ω_{ph} the renormalized phonon spectrum, χ the Pauli spin susceptibility of the electron–phonon interacting system, and χ_0 the Pauli spin susceptibility

* Corresponding author. Address: Dipart. di Fisica, Università di Roma 'La Sapienza', P.le A. Moro, 2, 00185 Roma, Italy. Tel.: +39 06 49913450; fax: +39 06 4463158.

E-mail address: emmcapp@roma1.infn.it (E. Cappelluti).

of non-interacting particle. For sake of simplicity we have here neglected possible effects of the electron–electron interaction U which, in the small correlation limit, would lead to an additional dependence on an electronic parameter $\mu = UN(0)$ in the right hand side of Eqs. (1)–(4). In this context, the search for high- T_c superconductivity in the 70’s was mainly aimed to look for strong coupling materials where the high T_c would stem from a large value of λ . Along this line the highest critical temperature ($T_c = 23$ K) was achieved for Nb_3Sn with a coupling $\lambda = 1.7$, and an empirical-theoretical upper limit $T_c^{\text{max}} \approx 20 - 25$ K was assumed to exist on the basis of optimization criteria and lattice stability considerations. The discovery of high- T_c superconductivity in cuprates ($T_c^{\text{max}} \approx 135$ K) [2] but also in fullerenes [3] and MgB_2 [4] ($T_c^{\text{max}} \approx 40$ K) points out thus in the most evident way the need of a deep revision of the above outlined framework.

Despite several different physical effects have been proposed as possible origins of the breakdown of the Migdal–Eliashberg scenario, there is still an open debate about the nature of the superconducting pairing mechanism in each family of materials, and the question whether there is a common physical origin of the high T_c , underlying all the different compounds, is still unsolved. An interesting suggestion along this perspective comes from the so-called Uemura’s plot [5] (Fig. 1) which shows that a common feature of all the unconventional superconductors is the small value of the Fermi energy $E_F = 0.1 \text{ cm}(5 \times 10^2 \text{ meV})$, one or more orders of magnitude smaller than the conventional low- T_c materials ($E_F \approx 10^4 \text{ meV}$).

Such small values of E_F strongly question the conventional ME Fermi liquid picture above discussed. On one hand the electronic kinetic energy becomes comparable to the electron–electron repulsion, $E_F \sim U$, leading to strong electronic correlation effects. This issue has been widely investigated, in particular in cuprates and C_{60} compounds, and, although its precise relation with the superconducting pairing is still debated, it is thought to be crucial in order to understand the phase diagrams of these materials.

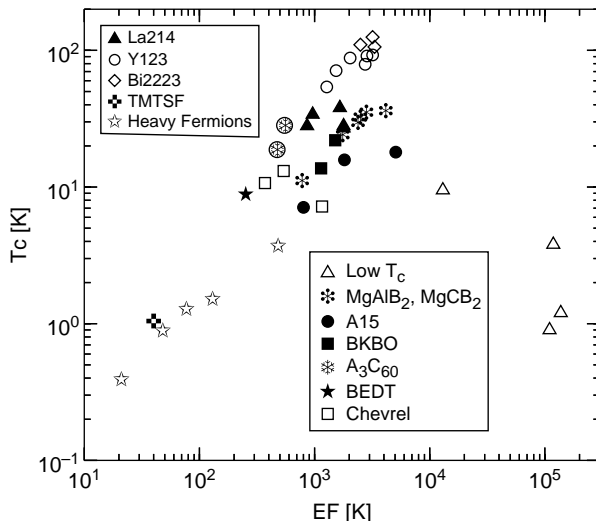


Fig. 1. Re-elaboration of T_c vs. E_F plot after Ref. [5] including fullerenes and magnesium diboride alloys.

Here, we would like to focus on a second source of breakdown of the conventional electron–phonon Fermi liquid picture, coming from the violation of the adiabatic assumption $E_F \sim \omega_{\text{ph}}$. In this regime indeed the separation between the energy scales of the electronic and lattice dynamics is no more operative and the corresponding electron and lattice degrees of freedom are strongly mixed. Extreme cases are the itinerant polaronic regime, described by the Lang–Firsov–Holstein approximation which is representative of the anti-adiabatic limit $\omega_{\text{ph}} \gg E_F$, and the self-trapped polaron picture which is valid in the almost adiabatic strong coupling regime. In our discussion we are more interested in the continuous evolution of nonadiabatic effects from the strictly adiabatic case $\omega_{\text{ph}}/E_F = 0$ to the weakly nonadiabatic regime $\omega_{\text{ph}}/E_F - 0.1 \text{ cm} \lesssim 1$ [6,7]. In this context a more useful starting point is the Migdal’s theorem that permits to identify a class of Feynman’s diagrams [6,7] which are responsible for non-adiabatic scattering processes and which can be introduced in a controlled way. More precisely, we can write a formally exact expression of the electronic self-energy as:

$$\sum_{\text{ph}}(k) = - \int dq G(k+q) D(q) I(k+q, q), \quad (5)$$

where G is the one-electron propagator, D the phonon Green’s function and I the total electron–phonon vertex function. It is often useful to split the total vertex function I into a zero order constant term plus higher order vertex corrections, denoted by P , namely:

$$I(k+q, q) = 1 + P(k+q, q). \quad (6)$$

The many-body nature of the electron–phonon problem is thus hidden in the unknown function I which in principle does not have an analytic expression. Migdal was able to show in the late 50’s [8] that the first order vertex correction P , shown in Fig. 2, scales to zero with the adiabatic ratio ω_{ph}/E_F , namely:

$$P(k+q, q) \propto \lambda \frac{\omega_{\text{ph}}}{E_F}, \quad (7)$$

where λ is the electron–phonon coupling constant. The analysis of the Migdal’s theorem permits to define a diagrammatic perturbation theory in terms of the adiabatic parameter ω_{ph}/E_F just by counting the number of vertex processes (Fig. 2(a)) implied in a skeleton expansion [6,7]. In the first order for instance the Green’s function will be related to the electronic self-energy Σ depicted in Fig. 2(b). Higher order response functions (e.g. superconducting, charge, spin susceptibilities) can be thus obtained in a consistent way as functional derivatives of Σ with respect to appropriate external fields, in the spirit of the conserving Baym–Kadanoff theory. The superconducting Cooper susceptibility for $T \approx T_c$ is shown for example in Fig. 2(c).

The inclusion of the nonadiabatic channels of interaction has important effects on the electron–phonon phenomenology of small Fermi energy systems. Most remarkable is the possible enhancement of the superconducting coupling in nonadiabatic materials [6,7] in the presence of strong electronic correlation

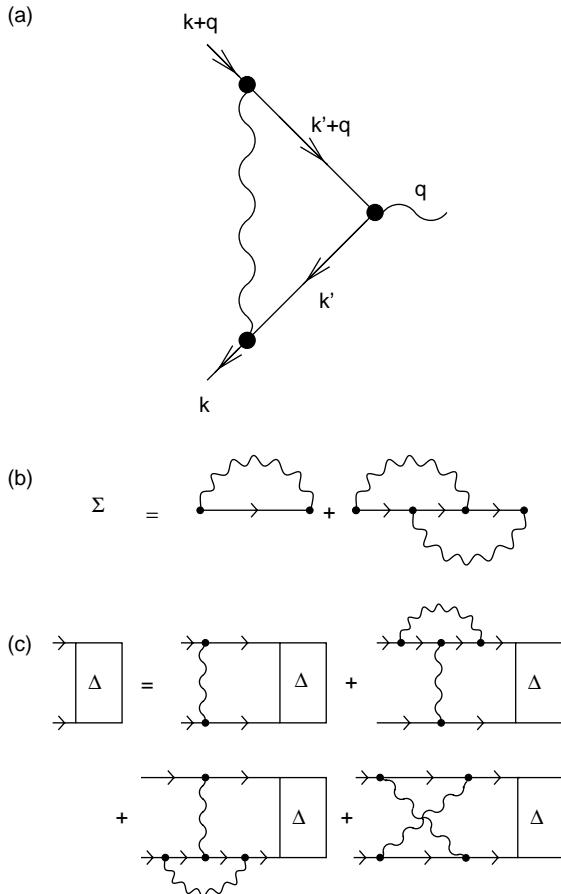


Fig. 2. (a) Diagrammatic representation of the first order electron–phonon vertex correction, (b) first order nonadiabatic self-energy.

where the approaching of a metal–insulator transition leads to a reduction of the screening properties and to a dominance of forward electron–phonon scattering [9–11]. Similar effects were also pointed out in Ref. [12]. In the following we shall focus mainly on normal state properties and we shall discuss the new perspectives arising from the nonadiabatic electron–phonon scenario in order to understand some unconventional features of the high- T_c compounds.

One of the most recently debated issues in cuprates is the occurrence of a kink in the electronic dispersion detected by angle-resolved photoemission spectroscopy (ARPES) techniques [13,14]. This feature is commonly discussed in terms of electronic renormalization of the band dispersion induced by some retarded bosonic degree of freedom. While the nature of such bosonic interaction is still not clear (phonons, spin or superconducting collective excitations, ...) the coarse grained interpretation is based on the conventional ME picture of the electron–phonon interaction generalized to a boson mediator with generic spectrum. In this framework the energy of the kink, E_{kink} , represents the characteristic energy scale of the spectrum, the high-energy dispersion $E_{\mathbf{k}}^{\text{high}} > E_{\text{kink}}$ gives the unrenormalized band-like dispersion $E_{\mathbf{k}}^{\text{high}} \approx \varepsilon_{\mathbf{k}}$, and the ratio between the low energy slope $E_{\mathbf{k}}^{\text{low}} > E_{\text{kink}}$ and $\varepsilon_{\mathbf{k}}$ estimates the overall coupling $\lambda = 1 - E_{\mathbf{k}}^{\text{high}}/E_{\mathbf{k}}^{\text{low}}$. A interesting point of this scenario is that in large Fermi energy systems different sources of scattering just

sum linearly in the electronic self-energy as far as E_F is larger than any bosonic energy scale involved. For the same reasons elastic scattering (for instance, impurities or disorder) is shown to not yield any renormalization of the electronic dispersion.

The above picture is drastically modified in small Fermi energy systems as cuprates where E_F can be of the same order of ω_{ph} (we discuss here these effects in terms of the electron–phonon interaction) [15]. A qualitative overview of the nonadiabatic novel effects is summarized in Fig. 3 where we plot the renormalized electronic dispersion for a small Fermi energy system ($E = 4\omega_{\text{ph}}$) (see the caption for details).

The small Fermi energy effects on the electron–phonon interaction alone is pointed out by comparing the $\gamma/\omega_{\text{ph}} = 0$ curve with the adiabatic limit. A crucial result is the prediction in small Fermi energy systems of an ‘anti-renormalization’ of high energy dispersion $E_{\mathbf{k}} > \omega_{\text{ph}}$ ($E_{\mathbf{k}} > \varepsilon_{\mathbf{k}}$) [15]. This implies that the slope inferred from the high-energy part of ARPES data will *over-estimate* the bare electronic dispersion while the effective coupling obtained by the magnitude of the kink will *under-estimate* the actual strength. In addition, due to the self-consistent behavior of the electronic self-energy, different scattering channels will mix nonlinearly reflecting the many-body nature of the processes. One example is the additional renormalization of the electronic dispersion due to disorder, which in the large E_F limit is not expected to be operative. The interplay between disorder and electron–phonon scattering gives rise to an enhancement of the ‘anti-renormalization’ at high energy, and to an apparent reduction of the electron–phonon coupling estimated by the renormalization of the low energy part. These results make thus quite questionable the conventional discussion of the ARPES data in terms of

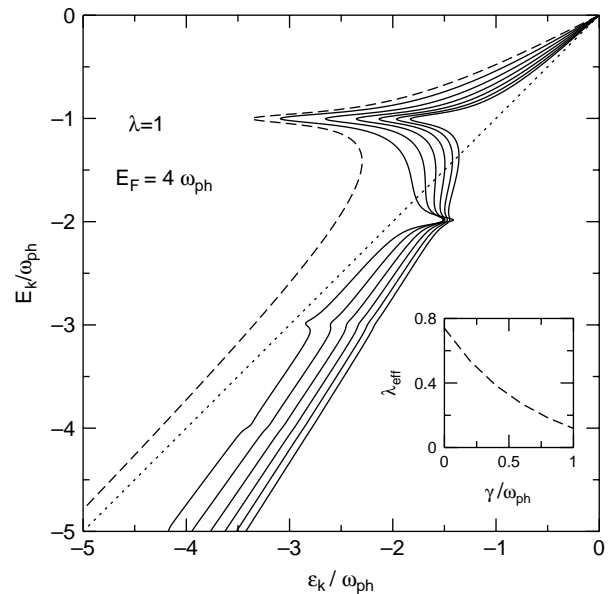


Fig. 3. Renormalized electron dispersion for a Einstein phonon mode with $\lambda = 1$ and $E_F = 4\omega_{\text{ph}}$ in the presence of impurity scattering. Solid lines corresponds to (from left to the right) $\gamma/\omega_{\text{ph}} = 0, 0.2, 0.4, \dots, 1.0$ where γ is the impurity scattering rate. The dashed line represents the adiabatic limit and the dotted one the bare (unrenormalized) dispersion. Inset: dependence of the effective parameter λ_{eff} on the impurity scattering rate.

a generalized ME theory for a generic boson excitation, pointing out the need of a more careful analysis which should take into account these nonadiabatic effects.

Spectroscopy techniques allows to investigate nonadiabatic effects by looking at unconventional features on the energy order of the phonon scale. Additional informations can be extracted by the study of unconventional electron–phonon properties on thermodynamical quantities. In particular, a powerful tool of investigation is the analysis of isotope effects on different quantities, since isotopic substitution directly probes the retarded nature of the electron–phonon interaction. In this context the experimental observation in cuprates of a finite isotope effect on the penetration depth [16], usually related to a finite and negative isotope effect on m^* , is quite interesting since these quantities are not expected to have any isotope effect within the framework of the conventional ME theory. Generally speaking, indeed, within the Fermi liquid picture of the ME theory for the electron–phonon interaction the isotope coefficient on a given observable A , $\alpha_A = -d \ln A/d \ln M_{\text{at}}$ ($= (1/2)d \ln A/d \ln \omega_{\text{ph}}$ since $\omega_{\text{ph}} \propto M_{\text{at}}^{-1/2}$ where $M_{\text{at}}^{1/2}$ is the atomic mass), is univocally determined by Eqs. (1)–(4), for

instance $\alpha_{m^*} = \alpha_{\chi} = 0$ and $\alpha_{T_c} = 0.5$ ($\alpha_{T_c} < 0.5$ if the Coulomb repulsion is taken into account).

In Fig. 4 we show the isotope coefficients α_{m^*} , α_{χ} evaluated within the nonadiabatic theory as functions of the adiabatic ratio ω_{ph}/E_F and of the electron–phonon coupling λ [17,18]. We find a finite and negative isotope effect for both m^* and χ , in qualitative agreement with the experimental measurements on the penetration depth for what concerns m^* . The observation of finite isotope effects comes from the onset of nonadiabatic scattering processes which lead to an additional dependence on ω_{ph} of these quantities, with significant deviations from the ME values. In this perspective, the prediction of a finite isotope effect on quantities, as m^* or χ , which are *not* expected to show it, is a novel feature which can be considered a direct evidence of a nonadiabatic character of the electron–phonon interaction. Experimental efforts in this direction are thus strongly suggested and welcome, to the aim of investigating anomalous isotope effects in particular on normal state quantities, and for instance the uniform Pauli spin susceptibility, NMR spin-lattice relaxation rate etc. Previous results showing puzzling isotope effect have been also reported in the ARPES dispersion curves in cuprates, with a sizable isotope effect on the *high-energy* part [19], where phonons, according to ME theory, are not expected to play any role. Experimental accuracy is however still too low to detect isotope shifts on the low energy part.

In the above discussion we have focused on two experimental tools, ARPES techniques and isotope substitutions, to detect anomalous electron–phonon features in small Fermi energy systems. As outlined, these techniques have been in particular applied with success in cuprates, where phonon energies range up to $\omega_{\text{ph}}^{\text{max}} \sim 70\text{--}80$ meV and $E_F \sim 300\text{--}350$ meV. In these materials, however, the electron–phonon coupling is known to compete with several other different interactions (electronic, magnetic, etc.) so that it is somehow difficult to isolate a single effect from the other ones. More promising candidates to detect nonadiabatic effects are thus the C_{60} -compounds where on one hand $\omega_{\text{ph}}^{\text{max}} \sim 200$ meV and $E_F \sim 250$ meV [20], so that the nonadiabatic ratio is one of the highest $\omega_{\text{ph}}^{\text{max}}/E_F \sim 0.8$, and where on the other hand many exotic features which are present in cuprates (stripes, pseudogap, magnetic correlations) are absent or very weak. Yet, in spite of such simplifications, the interplay of electron–phonon interaction with a significant electronic correlation and the Jahn-Teller nature of the H_g vibrational modes make the nonadiabatic phenomenology of these compounds quite interesting. In the last part of this contribution we would like thus to provide a brief discussion about possible multiband Jahn-Teller effects in the nonadiabatic phenomenology.

Electronic properties in fullerenes are strongly related to the t_{1u} C_{60} -molecular orbitals, which in the isolate molecule are threefold degenerate and which hybridize in the C_{60} solids to form the conduction bands in the A_3C_{60} family. Due to the electronic correlation, these superconductors are thought to be close to a metal-insulator transition on the metallic side [20]. The loss of their metallic and superconducting character for large intermolecular spacing constant a or for ammonia

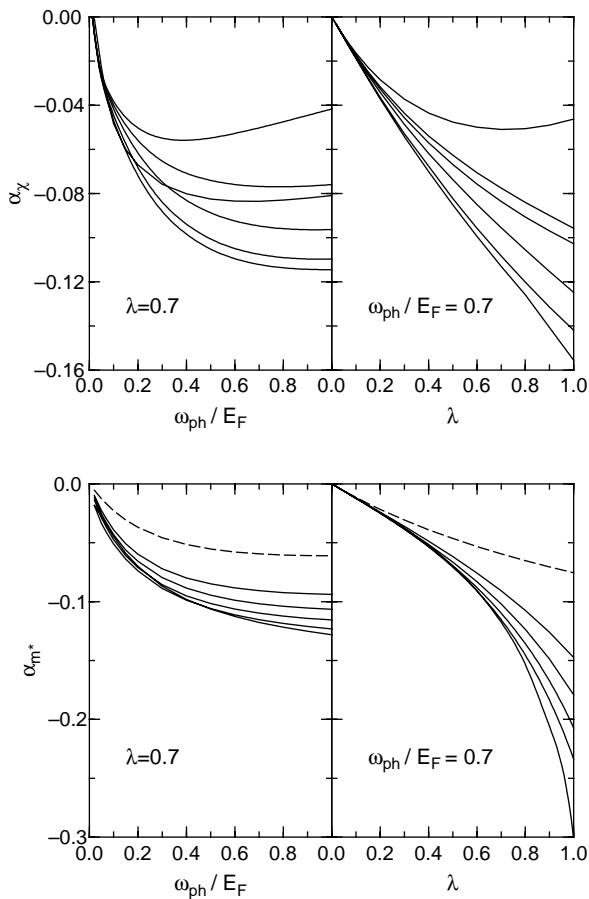


Fig. 4. Isotope effects on the effective electron mass m^* (top panel) and on the Pauli spin susceptibility χ (bottom panel) in the nonadiabatic theory. Dashed lines represent the isotope effects evaluated at the non-crossing approximation, where nonadiabatic effects are taken into account only by the finite bandwidth, solid lines are the full vertex corrected theory (different lines corresponds to different degrees of the electronic correlation; see Refs. [17,18] for more details).

intercalation is however always accompanied by a reduction of symmetry [21], suggesting that band-structure details are also important.

A widely used approach to investigate electron–phonon properties in fullerenes is the dynamical mean-field theory (DMFT) which does not rely on any small parameter expansion and which is in principle suitable for any strong coupling or strongly nonadiabatic regime. In order to provide a closed set of equations, the electron hopping term is often assumed to be diagonal within the space of the molecular orbital index, and the three bands are assumed to be degenerate. Within these constraints the superconducting properties of A_3C_{60} compounds in the presence of electronic correlation and electron–phonon interaction with H_g Jahn–Teller modes has been studied numerically [22,23]. As an interesting result, the conventional ME theory was found to be quite robust even for intermediate values of λ and ω_{ph}/E_F [23], where a nonadiabatic analysis would predict significant discrepancies.

The diagrammatic analysis of the nonadiabatic theory above presented permits to understand on the analytical ground the origin of the robustness of ME theory in multiband Jahn–Teller systems as a consequence of the assumption of *degenerate bands*. This is shown in the easiest way by looking at the vertex diagram depicted in Fig. 2(a). Assuming the electronic bands to be degenerate and diagonal in the molecular orbital space (but this result holds true even if not diagonal), one can show that [24]:

$$\Gamma(k + q, q) = 1 + \frac{1}{10}P(k + q, q), \quad (8)$$

to be compared with the single band non Jahn–Teller system (Eq. (6)). The reduction of the vertex processes by a factor 10 is simply due to the Jahn–Teller matrix structure of the electron–phonon scattering $\sum_\nu \hat{V}^\nu \hat{V}^\mu \hat{V}^\nu = (1/10)\hat{V}^\mu$, where μ, ν are indexes of the fivefold H_g modes and the matrices \hat{V}^μ live in the 3×3 molecular orbital space.

We would like to stress that the above result strongly relies on the assumption of degenerate t_{1u} electronic bands. This assumption is however questionable in A_3C_{60} materials where the inter-molecular hybridization in the fcc structure and the orientational order of the buckyballs can significantly affect the band structure. The sensibility of the band-like structure to these features as well as to possible crystal field splitting (as induced by ammonia intercalation) could thus account for anomalous metal–insulator transitions accompanied by the loss of symmetry properties in large unit cell fullerenes and in ammonia intercalated compounds.

In order to assess in a more realistic way the role of the multiband Jahn–Teller effects in A_3C_{60} family we consider thus a one-directional tight-binding (TB) model for the t_{1u} bands as discussed in Ref. [25] which reproduces first-principle LDA calculations with a high degree of precision. The electronic band structure along the high-symmetry axes of the fcc Brillouin zone and the total electron DOS has been widely reported in literature [20]. It should be noted that the (low energy) electronic

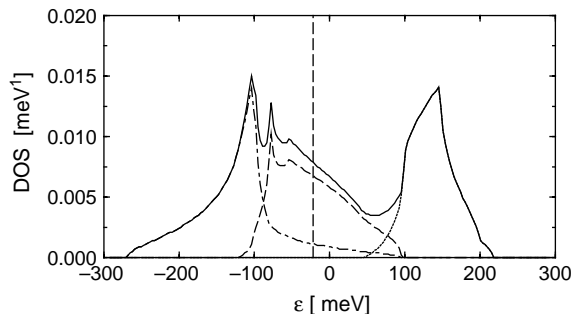


Fig. 5. Total DOS and partial DOS for each electronic band in the one-directional TB model for A_3C_{60} . The dashed vertical line represents the Fermi level μ .

and transport properties are mainly determined by quantities defined at the Fermi level, as the Fermi surface itself, the electron DOS at the Fermi level, the Fermi velocity, etc. A realistic band structure can thus be modeled as a degenerate three-band system only if it presents qualitatively similar Fermi sheets, with similar densities of states and similar Fermi velocities. In this perspective A_3C_{60} compounds seems not to be a good candidate since it is known to have only two Fermi cuts of the electronic bands with quite different Fermi surfaces [26]. A more quantitative analysis comes from decomposing the total DOS in the single contributions from each band. A plot of the total DOS along with its components is plotted in Fig. 5 which shows that the electronic band structure is largely dominated at the Fermi level by a single band which is roughly half-filled, with two additional bands which are quite far from the Fermi level. Generally speaking, these bands would not significantly contribute to interband electron–phonon scattering as long as the phonon energy is not large enough to trigger high-energy processes involving the main part of their DOS. Detailed calculations show indeed that for realistic phonon energy ($\omega_{ph} \leq 200$ meV) more than 50% of the electron–phonon scattering comes from intraband processes [24] suggesting that a single band non Jahn–Teller model could be a better starting point to describe electron–phonon properties in these materials than a three degenerate band model. Note that similar considerations do not apply to the Coulomb–Hubbard repulsion where no small energy scale is present and electron scattering involves, in principle, high energy as well as low energy excitations.

References

- [1] G. Grimvall, *The Electron–Phonon Interaction in Metals*, North-Holland, Amsterdam, 1981.
- [2] J.G. Bednorz, K.A. Müller, *Z. Phys. B* 64 (1986) 189.
- [3] A.F. Hebard, et al., *Nature* 350 (1991) 600.
- [4] J. Nagamatsu, et al., *Nature* 410 (2001) 63.
- [5] Y.J. Uemura, et al., *Nature* 352 (1991) 605.
- [6] L. Pietronero, et al., *Phys. Rev. B* 52 (1995) 10516.
- [7] C. Grimaldi, et al., *Phys. Rev. B* 52 (1995) 10530; C. Grimaldi, et al., *Phys. Rev. Lett.* 75 (1995) 1158.
- [8] A.B. Migdal, *Sov. Phys. JETP* 7 (1958) 996.

- [9] R. Zeyher, M.L. Kulić, *Phys. Rev. B* 53 (1996) 2850.
- [10] M.L. Kulić, *Phys. Rep.* 338 (2000) 1.
- [11] M. Grilli, C. Castellani, *Phys. Rev. B* 50 (1994) 16880.
- [12] M.S. Osofsky, et al., *Phys. Rev. Lett.* 87 (2001) 197004; M.S. Osofsky, et al., *Phys. Rev. B* 66 (2002) 020502.
- [13] A. Lanzara, et al., *Nature* 412 (2001) 510.
- [14] X.J. Zhou, et al., *Nature* 423 (2003) 398.
- [15] E. Cappelluti, L. Pietronero, *Phys. Rev. B* 68 (2003) 224511.
- [16] R. Kashanov, et al., *J. Phys.: Condens. Matt.* 16 (2004) S4439.
- [17] C. Grimaldi, et al., *Europhys. Lett.* 42 (1998) 667.
- [18] E. Cappelluti, et al., *Phys. Rev. B* 64 (2001) 025136.
- [19] G.-H. Gweong, T. Sasagawa, S.Y. Zhou, J. Graf, H. Takagi, D.-H. Lee, A. Lanzara, *Nature* 430 (2004) 187.
- [20] For a review see O. Gunnarsson, *Rev. Mod. Phys.* 69 (1997) 575.
- [21] Y. Iwasa, T. Takenobu, *J. Phys.: Condens. Matter* 15 (2003) 495.
- [22] M. Capone, et al., *Science* 296 (2002) 2364.
- [23] J.E. Han, et al., *Phys. Rev. Lett.* 90 (2003) 167006.
- [24] E. Cappelluti, et al., *Phys. Rev. B* 72 (2005) 054521
- [25] S. Satpathy, et al., *Phys. Rev. B* 46 (1992) 1773.
- [26] S.C. Erwin, W.E. Pickett, *Science* 254 (1992) 842.